



Islamic Azad University
Mashhad Branch

Source Rock evaluation, Modelling, Maturation, and Reservoir characterization of the Block 18 oilfields, Sab'atayn Basin, Yemen

A.S. Alaug^{1*}, D. Leythäuser², B. Bruns² and A.F. Ahmed¹

1. Taiz University, Faculty of Applied Sciences, Geology Department, Taiz 6803, Yemen.

2. RWTH Aachen University, Inst. of Geology and Geochemistry of Petroleum and Coal, Germany.

Received 15 May 2011; accepted 13 October 2011

Abstract

A total of 183 core and cutting samples from seven exploratory wells were selected to be analyzed by Rock-Eval pyrolysis. These cores have been drilled through the Lam and Meem Members of the Madbi Formation and contain the major source rocks of Yemen's sedimentary basins. Contents of total organic carbon were measured and Rock-Eval pyrolysis was performed to evaluate the hydrocarbon potential of Block 18 oilfields in central Yemen. Most of the studied samples have fair to excellent petroleum generation potential as shown by the results of PP, PI, HI and TOC. They have also sufficient TOC values with an average value of 1.48 wt% and a maximum value of 12.34 wt% with a good petroleum potential averaging 4.54 kg HC/ton of rock and a maximum value of 44.78kg HC/ton of rock. HI values of the Madbi Formation in its full thickness range from 16 mg to 1114 mg HC/g TOC with an average value of 273 mg HC/g TOC. Kerogen types II and III, and a small amount of type I can be observed. These kerogens are thermally mature and mostly within the hydrocarbon generation zone. In a numerical simulation approach the thermal and burial history of the Alif-1 well, which is representative for this area was modelled. Using vitrinite reflectance data, as means of calibration, the modelling results were subjected to a sensitivity analysis concerning paleo-heat flow, radiogenic heat production, basement thickness and eroded overburden or maximum burial, respectively. The calculated temperature during deepest burial of the source rock layers of the Madbi Formation reached 158 °C for the Lam Member and 182 °C for the Meem Member. Compliance with the measured R_0 values, used as calibration parameter, could be achieved by assuming an erosion of 1100 m of the Upper Tawilah Group. The heat flow is maximized at the onset of basin rifting in Late Jurassic to 90 mW/m² having a base level of 60 mW/m². Thus, the Lam Member has reached the main oil to wet gas window at its deepest burial whereas the Meem Member has undergone the wet gas window in its full thickness. The isopach map of the Alif Member, as the main reservoir in the studied area, indicates thickening of the sandstone unit towards the eastern and western parts of Block 18 around the Dostour Al-Wahdah gasfield in the east and at the Alif oilfields in the west.

Keywords: Maturation, Hydrocarbon potential, Modelling, Petromod, Madbi formation, Alif member, Block 18, Yemen.

1. Introduction

The earliest exploration for hydrocarbons in Yemen was commenced in 1961 within the Red Sea coastal region. However, the first commercial discovery was made in 1984 in the Block 18, Marib sub-basin, Sab'atayn Basin in the central part of the Republic of Yemen (Fig.1a). Yemen entered the era of oil in the summer of 1984 when the Yemen Hunt Oil Company announced the first commercial discovery of oil in the Alif field (Fig.1). The Alif-1well started with a production rate of 8000 BOPD. Since that time several oil and/or gas fields were discovered in Block 18 (Fig.1b). Meanwhile, development of Block 18 was carried out through construction of a pipeline to the Red Sea. In September 1986 the production and export of the first oil shipment from Block 18 was executed.

*Corresponding author.

E-mail address (es): wahabalaug@Yahoo.com

In 1987 oil discoveries were announced by Technoexport, a former Russian oil company, in several fields in the Shabwa sub-basin. In September 1996 oil was discovered in the Halewah oilfield, Block 5, in the Sab'atayn Basin (Fig. 1b). It was discovered by a consortium of companies operating in this block. In 2003 the Vintage Petroleum Company announced another commercial oil discovery within Block S1. There are 36 discoveries in the Sab'atayn Basin with the estimated resource of the Alif reservoir reaching to almost 1.7 billion barrels of oil and condensate as well as 18 trillion cubic feet of gas. The clastics and evaporites of the Sab'atayn Formation are providing the reservoir and regional seal within the Marib and Shabwa sub-basins. The major reservoir was recognized in the Alif Member and in the Yah, Seen and Safer Members as minor reservoir units in blocks 18, 5, 4 and S1 (Figs. 1-2). Further activity spread to the southern and eastern parts of the Republic of Yemen with a series of discoveries made by different

petroleum companies from the early 1990's until now.

2. Geological Setting

The geological evolution of Yemen was driven by the plate motions that broke southern Gondwana apart in the Mesozoic and formed the Gulf of Aden and Red Sea in the Cenozoic. The stratigraphy and regional geology of Yemen was established by several workers [1, 2, 3, 4, 5, 6, 7, 8, 9, 10, 11, 12, 13 and 14]. Hydrocarbon exploration activity increased extensively after 1984 and provided considerable amounts of subsurface data such as the work of [13, 15, 16, 17, 18, 19, 20, 21 and 22] which allowed a revised synthesis of the basin evolution in Yemen. Only a few publications have addressed the geology and petroleum geology of the Sab'atayn Basin which is a comparatively poorly-studied basin [13, 15, 22, 23, 24, 25 and 26].

The interior rift basins of Yemen were formed as a result of the Late Jurassic rifting between East Africa and western India [15, 16 and 18]. The Sab'atayn Basin, as a major Mesozoic rift basin of Yemen, comprises several sub-basins which are from northwest to southeast Al-Jawf, Marib and Shabwa (Fig. 1a). The Sab'atayn Basin is 50–120 km wide and more than 450 km long (Fig. 1a). The stratigraphic column in the Sab'atayn Basin is dominated by a thick Mesozoic succession with an average thickness reaching up to 2500 m (Fig. 2). The oldest sediments within the northern and north-western parts of the Sab'atayn Basin are of Palaeozoic age (Wajid and Akbarah formations). The Wajid and Akbarah Formations are only recorded as subsurface occurrences in the northern part of the Sab'atayn Basin, particularly within the Al-Jawf sub-basin, and the Akbarah Formation occurs in the north-western part of the Marib sub-basin but with limited extension [13, 21 and 27] (Fig. 2). During the early to middle Jurassic time the Kuhlan Formation was deposited and preserved in small intra-basinal lows surrounded by broad Late Jurassic platforms [8, 10 and 28]. This formation is not recorded in most of the central parts of the Sab'atayn Basin (Fig. 2). The pre-rift phase sequences in the basin are represented by the Wajid, Akbarah, and Kuhlan Formations (Fig. 2). The Kuhlan Formation is conformably grading upwards into the platform carbonates of the Shuqra Formation. The Marib and Shabwa sub-basins were dominated by filling of the Amran Group sequences as a result of the first major NW-SE oriented rifting phase which included Shuqra, Madbi, Sab'atayn and Nayfa Formations (Fig. 2). The Shuqra Formation was deposited during Bathonian/Callovia-Oxfordian time as a result of the early-rift phase events. The syn-rifting phase created horst and graben structures which provide the organic rich sediments of the Madbi Formation (Fig. 2). The syn-rift phase strata within the Sab'atayn Basin are of Kimmeridgian age with maximum subsidence and

sedimentation rates occurring in this time [15]. The late syn-rift phase events during Tithonian time caused the formation of the thick sequence of clastic and evaporite sediments of the Sab'atayn Formation (Fig. 2). The Marib and Shabwa sub-basins were isolated and filled with fluvial-deltaic to shallow-nearshore clastics and evaporites of this formation during late-rift phase events [13 and 22]. Madbi and Sab'atayn Formations constitute the source, reservoirs and seal rocks of the Marib and Shabwa sub-basins [22, 23 and 24]. The Nayfa Formation is formed by the post-rift phase events during the Late Tithonian to Early Berriasian time (Fig. 2). The Tawilah group sediments were predominantly deposited by the second major NW-SE oriented rifting phase of the Sab'atayn Basin during Cretaceous time (Figs. 1a; 2).

This study is mainly focused on the main source rocks of the Madbi Formation, which consists of argillaceous strata with porous lime-grainstone to argillaceous lime-mudstone. The lithofacies represents deposition within an open marine to shallow marine environments. Increased organic content indicates restricted basin conditions with anoxic bottom waters [27]. This succession is classified into two lithostratigraphic units [13, 21 and 29]. The lower unit, Meem Member, is commonly made up of argillaceous limestone whereas the upper one, Lam Member, is composed of laminated organic-rich shale, mudstone, and calcareous sandstone and is a prolific source rock in the Sab'atayn Basin (Fig. 2). Both of these have organic-rich black shale deposited in the deeper portions of the Marib sub-basin. Therefore, they are considered to represent the main source rocks among all the productive sedimentary basins of Yemen.

3. Materials and Methods

In this paper maturation and hydrocarbon potential of Block 18 oilfields, Marib sub-basin, Sab'atayn Basin, central Yemen, are evaluated on the basis of organic geochemical analysis and are complemented by calibration parameters, basin modelling and its interpretation (Figs. 1a-b). In all, 183 core and cutting samples were selected and prepared from seven wells of Block 18 oilfield, Marib sub-basin, for organic geochemical analysis by the author [27]. These samples of the Meem and Lam Members of the Madbi Formation came from 7 onshore exploratory wells of Block 18 oilfields (Table 1). Out of this total, 129 samples came from the Lam Member and 54 samples from the Meem Member (Table 1). The studied wells are Alif-1, Tawilah-1, AI-1, Meem-1, Salah Al-Deen, J. Haddan-1 and Kamaran-1 (Fig. 1b). For the source rock and hydrocarbon potentiality evaluation Rock-Eval pyrolysis and Total Organic Carbon (Py/TOC) measurements have been used. Standard Rock-Eval pyrolysis methodology [30, 31, 32 and 33] was used for the analyses.

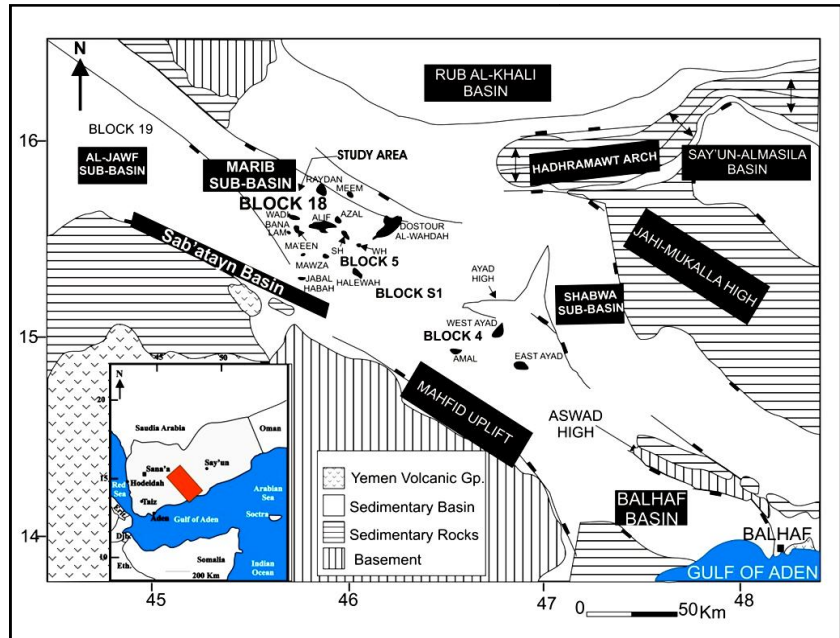


Fig. 1a. Simplified map of the Sab'atayn Basin and study area (modified after [22]).

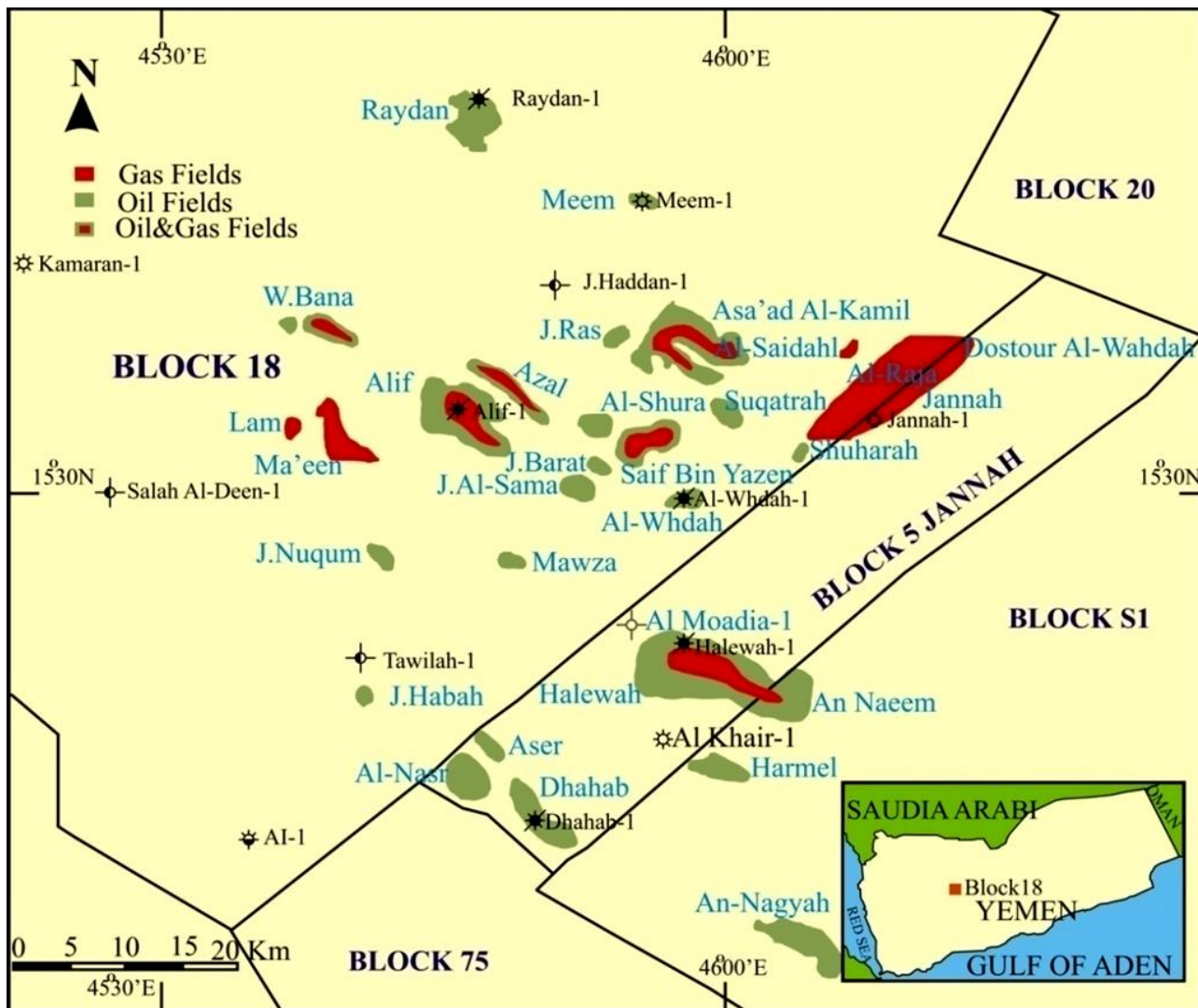


Fig. 1b. Simplified location map of the studied wells, oil and gas fields in Block 18 oilfields of the Sab'atayn Basin, central Yemen.

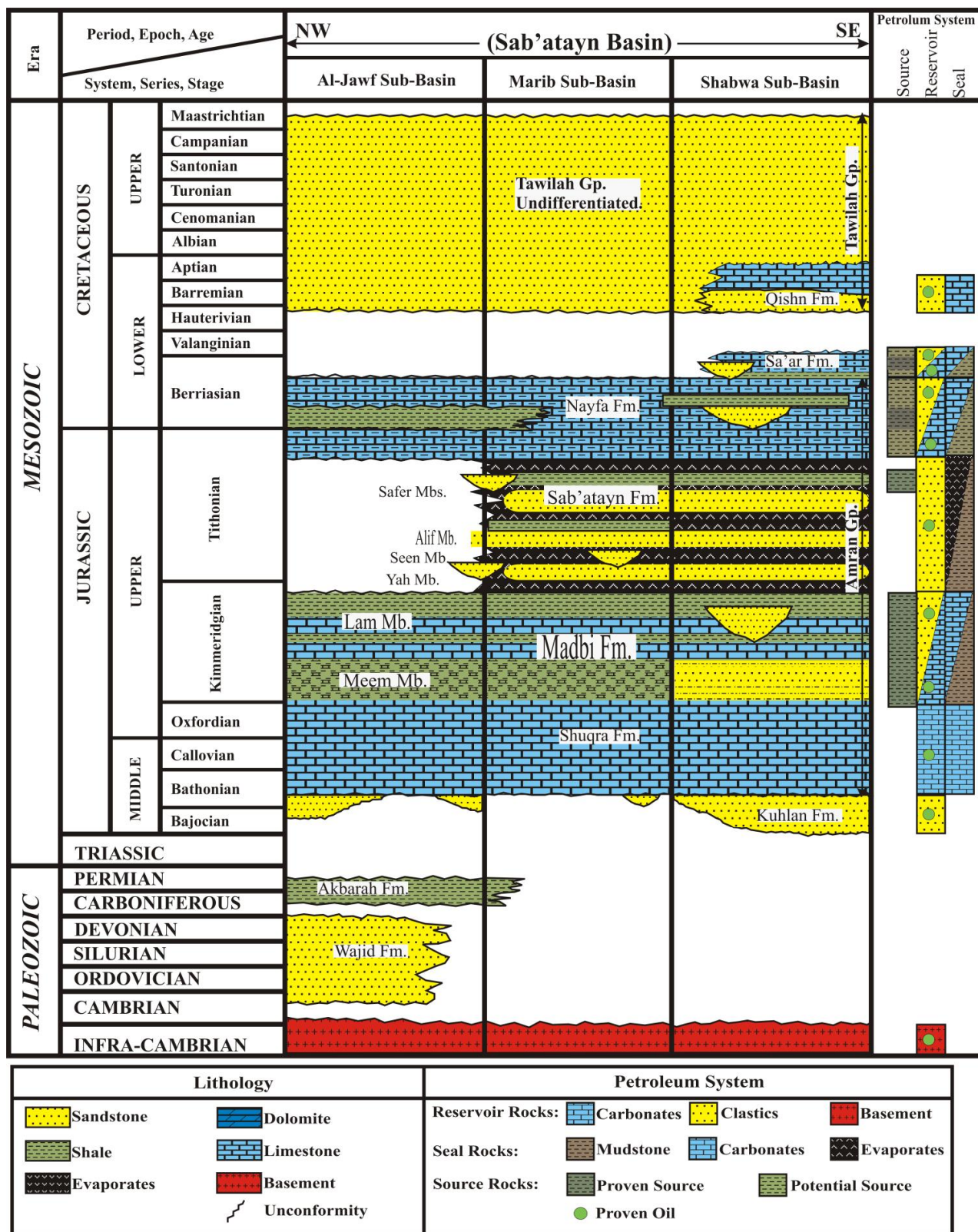


Fig. 2. Lithostratigraphic chart of the Sab'atayn Basin with a summary of the petroleum system elements (modified after [18, 21 and 45]).

Table 1. Rock-Eval pyrolysis/TOC results of the studied wells of Block 18 oilfields, Sab'atayn Basin.

Well	Member	Depth (m)	HI	OI	PI	T _{max}	TOC	S2	PP
Alif-1	Lam Member	1764	344	51	0.17	431	1.31	3.75	4.52
		1844	335	47	0.12	432	1.85	5.06	5.77
		1932	213	77	0.19	432	0.77	1.6	1.97
		2020.5	250	47	0.19	435	0.88	1.9	2.34
		2082	245	48	0.22	436	1.03	2.13	2.73
		2170.5	206	77	0.33	434	1.08	1.65	2.47
		2223.5	195	46	0.20	436	0.96	1.54	1.92
		2288	186	25	0.18	437	1.44	2.18	2.66
		2376	243	69	0.23	440	1.76	2.79	3.6
		2414.7	187	38	0.23	441	1.24	1.48	1.92
		2485	190	46	0.26	443	2.04	2.41	3.27
		2555.8	141	45	0.27	443	1.05	1.13	1.55
		2608	118	55	0.30	433	0.94	1.11	1.58
		2682	136	65	0.31	445	1.15	1.56	2.27
	Average	213.50	52.57	0.21	437.00	1.25	2.16	2.76	
	Meem Member	2735	121	98	0.3	439	0.8	0.7	1
		2742.6	71	35	0.42	436	0.71	0.45	0.78
		2808.8	110	39	0.34	458	0.3	2.39	3.6
		2897	100	40	0.29	455	0.56	2.4	3.4
		2950	55	142	0.41	445	0.93	0.36	0.61
		3038	40	68	0.46	424	0.98	0.27	0.5
		3111.7	52	65	0.52	369	0.93	0.37	0.77
		3164.7	40	25	0.46	334	1.6	0.29	0.54
3217.6		37	68	0.42	340	1.43	0.36	0.62	
3288		33	37	0.4	224	1.29	0.29	0.48	
3344		32	48	0.51	428	1.45	0.31	0.63	
Average	62.82	60.45	0.41	395.64	1.00	0.74	1.18		
Tawilah-1	Lam Member	Depth (m)	HI	OI	PI	T _{max}	TOC	S2	PP
		961	417	60	0.12	428	1.08	3.19	3.63
		1032	485	42	0.13	425	1.03	3.44	3.96
		1058	531	33	0.11	425	2.01	7.21	8.06
		1085	840	28	0.09	426	2.55	10.69	11.81
		1138	933	24	0.1	424	3.87	16.61	18.49
		1173	820	23	0.12	426	3.24	11.52	13.11
		1217	894	15	0.11	428	4.62	17.43	19.61
		1252	1114	12	0.17	441	5.9	26.14	31.52
	Average	754.25	29.63	0.12	427.88	3.04	12.03	13.77	
	Meem Mb.	1270	690	20	0.23	433	12.34	33.1	43.26
		1305	242	80	0.2	431	1.23	2.3	2.85
		1341	594	25	0.13	432	6.66	27.9	32.16
		1350	487	35	0.14	431	3.86	13.2	15.4
		1367	323	50	0.18	433	1.53	3.59	4.36
		1429	577	10	0.16	438	2.73	37.6	44.78
		Average	485.50	36.67	0.17	433.00	4.73	19.62	23.80
Meem-1	Lam Member	Depth (m)	HI	OI	PI	T _{max}	TOC	S2	PP
		1089	383	30	0.1	424	3.15	11.57	12.93
		1182	259	48	0.2	426	0.81	2.7	3.36
		1261	327	19	0.1	425	1.17	3.6	3.98
		1323	234	35	0.18	427	0.72	1.66	2.02
1382	139	15	0.15	482	2.79	3.81	4.5		

J. Hadan-1		1411	235	22	0.12	429	1.5	3.45	3.91	
		1438	365	17	0.09	422	2.77	9.28	10.17	
		1535	379	21	0.09	426	1.95	6.71	7.41	
		Average	290.13	25.88	0.13	432.63	1.86	5.35	6.04	
	Meem Member	1740	238	26	0.09	428	3.4	7.96	8.78	
		1835	118	31	0.15	435	1.4	1.18	1.39	
		1870	98	54	0.17	437	0.86	0.8	0.96	
		1950	170	28	0.16	437	1.21	1.96	2.33	
		1985	158	25	0.18	438	1.2	1.53	1.86	
		2029	128	41	0.19	437	0.73	0.88	1.08	
		2132	142	21	0.21	440	1.36	1.81	2.28	
		Average	150.29	32.29	0.16	436.00	1.45	2.30	2.67	
		Lam Member	Depth (m)	HI	OI	PI	T_{max}	TOC	S2	PP
			1811	325	30	0.13	433	1.53	4.17	4.77
	1832		134	50	0.25	436	0.54	0.69	0.92	
	1850		178	60	0.16	433	0.55	0.93	1.11	
	1870		149	63	0.23	434	0.6	0.85	1.11	
	1891		215	42	0.19	433	0.78	1.59	1.97	
	1911		120	104	0.28	432	0.49	0.56	0.78	
	1961		174	101	0.21	435	0.76	1.25	1.58	
1966	348		24	0.16	435	2.74	7.78	9.22		
1982	203		52	0.15	433	0.77	1.47	1.72		
2020	274		99	0.19	432	0.73	1.58	1.95		
2038	200		67	0.22	436	1	1.86	2.37		
2052	567		15	0.09	432	4.45	16.95	18.62		
2055	232		57	0.3	436	0.47	1.01	1.45		
2056	229		47	0.21	433	1.04	2.21	2.79		
2057	189		81	0.36	437	0.32	0.56	0.88		
2058	596		15	0.12	426	3.85	15.33	17.4		
2059	642		16	0.06	433	5.83	25.1	26.78		
2060	788		20	0.07	430	4.25	22.33	23.95		
2061	304		72	0.1	437	1.39	3.14	3.48		
2062	226		70	0.18	439	0.79	1.65	2		
2063	118		129	0.34	433	0.25	0.23	0.35		
2064	305		74	0.13	433	1.1	2.36	2.7		
2065	310		49	0.13	437	1.73	4.12	4.71		
2066	462		29	0.11	436	1.94	5.92	6.62		
2067	40		243	0.31	432	0.31	0.11	0.16		
2068	304		32	0.15	435	0.13	3.19	3.76		
2073	291		45	0.14	438	0.96	2.14	2.5		
2085	218		34	0.11	437	1.69	3.38	3.79		
2091	153		70	0.13	438	0.71	1.1	1.27		
2108	170		66	0.2	437	0.71	1.1	1.38		
2126	266		48	0.18	437	1.19	2.33	2.84		
2144	210		57	0.17	440	1.11	2.11	2.55		
2161	204		43	0.16	438	1.23	2.26	2.68		
2187	678	18	0.09	433	3.89	14.72	16.12			
2200	129	56	0.25	439	1.01	1.16	1.55			
2217	145	50	0.2	439	1.11	1.42	1.78			
2235	144	73	0.32	441	0.83	1.05	1.54			
2255	222	22	0.17	438	3.17	6.12	7.41			
2270	213	38	0.02	441	1.76	3.24	3.31			
2282	545	16	0.1	440	5.97	15.4	17.17			
2288	155	54	0.22	441	1.47	1.96	2.52			

		2323	114	59	0.26	443	0.92	0.89	1.21
		2341	220	40	0.19	442	1.54	2.84	3.51
		2345	58	132	0.38	445	0.41	0.2	0.32
		2358	461	35	0.16	444	2.47	4.65	5.55
		2376	309	74	0.25	443	1.14	2.04	2.71
		2385	577	24	0.15	442	5.02	11.15	13.17
		2394	177	47	0.21	444	1.24	1.79	2.27
		2399	220	49	0.2	444	1.52	2.72	3.42
		2411	174	68	0.21	443	0.66	0.93	1.18
		2429	157	98	0.3	444	0.55	0.69	0.98
		2447	152	36	0.19	446	1.07	1.29	1.6
		2482	180	80	0.28	446	0.86	1.2	1.66
		2500	168	80	0.27	441	0.56	0.72	0.98
		2517	203	70	0.31	443	0.81	1.24	1.81
		2523	220	23	0.24	449	2.86	4.72	6.24
		2535	198	53	0.28	446	0.98	1.43	1.98
		2553	237	36	0.25	448	1.34	2.33	3.1
		2570	353	70	0.26	443	1.02	1.62	2.19
		2588	150	57	0.29	440	1	1.07	1.51
		2605	604	33	0.2	448	0.12	4.62	5.76
		2623	183	43	0.22	447	1.2	1.52	1.95
		2641	184	53	0.22	446	0.58	0.73	0.93
		2658	194	36	0.27	450	0.76	0.99	1.35
		2676	172	30	0.23	450	0.82	0.93	1.2
		2694	167	32	0.25	449	1.07	1.16	1.55
		2711	151	37	0.26	449	0.79	0.76	1.03
		2729	225	36	0.26	450	1.06	0.84	1.13
		2747	557	35	0.2	442	2.03	1.61	2.02
		2764	269	34	0.28	452	1.06	0.94	1.3
		2782	156	34	0.31	451	0.89	0.82	1.18
		2800	563	27	0.28	453	2.11	1.42	1.97
		2817	619	27	0.23	443	1.59	1.11	1.44
		2835	262	32	0.31	450	0.74	0.56	0.81
		Average	270.4	53.4	0.2	440.2	1.4	3.4	3.9
	Meem Member	2853	270	33	0.3	447	0.87	0.66	0.94
		2870	173	24	0.27	442	0.71	0.64	0.88
		2888	132	20	0.33	442	0.66	0.45	0.67
		2902	194	55	0.27	432	0.87	0.43	0.59
		2905	257	27	0.24	440	0.98	0.67	0.88
		2906	188	84	0.29	427	0.74	0.35	0.49
		2922	152	76	0.33	458	1.24	0.46	0.69
		2923	239	37.5	0.09	456	1.07	0.62	0.68
		2941	618	22	0.27	458	2.27	1.02	1.4
		2955	263	22	0.6	453	1.28	0.76	1.9
		2958	202	25	0.32	459	2.25	1.1	1.49
		2962	265	29	0.04	455	1.09	6.63	6.93
		Average	246.08	37.88	0.28	447.42	1.17	1.15	1.46
Kamran-1	Lam Member	Depth (m)	HI	OI	PI	T_{max}	TOC	S2	PP
		888	131	188	0.14	433	1.3	1.69	1.96
		1170	119	214	0.25	429	0.64	0.76	1.01
		1269	132	71	0.18	432	0.77	1.03	1.25
		1329	106	131	0.24	431	0.68	0.72	0.95
		1464	113	82	0.22	436	0.68	0.77	0.99
	1561	84	155	0.26	437	0.74	0.62	0.84	

		1667	154	56	0.21	440	0.7	1.08	1.37	
		1800	92	27	0.27	439	0.78	0.72	0.99	
		1932	149	29	0.27	444	0.87	1.3	1.77	
		2073	127	33	0.27	447	0.83	1.05	1.44	
		Average	120.7	98.6	0.231	436.8	0.799	0.974	1.257	
	Meem Member	2241	108	65	0.36	436	0.81	0.68	1.06	
		2479	29	36	0.5	474	1.03	0.21	0.42	
		2585	28	57	0.48	444	0.77	0.15	0.29	
		2647	26	57	0.48	435	0.79	0.14	0.27	
		2744	27	62	0.54	432	0.88	0.16	0.35	
		2841	34	79	0.51	359	1.03	0.24	0.49	
		3000	15	51	0.69	422	1.01	0.1	0.32	
		3150	22	63	0.51	354	1.13	0.7	1.42	
		3300	16	47	0.63	401	1.06	0.11	0.3	
3435		24	64	0.56	367	1.14	0.18	0.41		
3560	19	56	0.64	377	1.11	0.14	0.98			
Average	39.06	61.30	0.51	411.48	0.96	0.32	0.63			
Salah Al-Deen-1	Lam Member	Depth (m)	HI	OI	PI	T_{max}	TOC	S2	PP	
		1650	201	20	0.22	405	1.2	2.4	3.1	
		1710	190	21	0.29	400	1	1.9	2.7	
		1790	210	18	0.25	410	1.1	2.3	3.1	
		1870	199	25	0.25	406	0.7	1.45	1.95	
		Average	200	21	0.25	405	1	2.0	2.7	
	Meem Member	1950	227	22	0.24	410	0.8	1.82	2.4	
		2064	207	25	0.2	421	0.9	1.99	2.49	
		2130	156	34	0.12	442	0.66	1.38	1.58	
		2180	197	33	0.1	435	1.03	2.03	2.28	
		2204	204	18	0.07	394	1.01	2.1	2.27	
		Average	198.2	26.4	0.15	420.4	0.88	1.86	2.20	
	AI-1	Lam Member	Depth (m)	HI	OI	PI	T_{max}	TOC	S2	PP
			1100	442	130	0.37	421	0.7	3.1	4.9
1150			233	140	0.42	422	0.9	2.1	3.6	
1190			409	80	0.34	427	1.1	4.5	6.8	
1220			411	95	0.40	430	0.9	3.7	6.2	
1300			448	110	0.27	432	1.85	8.3	11.4	
1350			371	112	0.34	437	1.75	6.5	9.9	
1400			387	90	0.26	430	1.83	7.1	9.6	
1500			432	95	0.28	435	1.92	8.3	11.5	
1600			333	120	0.40	438	1.86	6.2	10.3	
1700			490	114	0.39	441	1.1	5.4	8.9	
Average		395.6	108.6	0.34	431.3	1.391	5.52	8.31		
Meem Member		1750	175	110	0.60	440	1.2	2.1	5.3	
		1800	545	113	0.44	442	1.1	6	10.7	
	1850	538	95	0.39	445	1.3	7	11.4		
	Average	419.3	106.0	0.45	442.3	1.2	5.0	9.1		

The Py/TOC measurements were done on organic rich samples using a Rock-Eval 6 instrument [31, 34 and 35]. This technique provides four fundamental parameters in which S1 represents free and adsorbed hydrocarbons, S2 shows pyrolysis generated hydrocarbons, S3 provides CO₂ released during the pyrolysis phase of the analysis, and T_{max} gives the

temperature of maximum pyrolytic hydrocarbon yield in °C. These fundamental parameters are used to deduce the values of TOC wt%; Hydrogen Index (HI=S2/TOC×100, in mg HC/g TOC); Oxygen Index (OI= S3/TOC×100, in mg CO₂/g TOC); Petroleum Potential (PP=S1+S2, in mg HC/g of rock or kg HC/ton of rock) and Production Index (PI=S1/S1+S2,

in mg HC/g of rock or kg HC/ton of rock). The precision of these parameters are $\pm 0.1\%$ for TOC; $\pm 1^\circ\text{C}$ for T_{max} ; ± 10 mg HC/g TOC for HI; ± 5 mg CO_2/g TOC for OI; ± 1 mg HC/g of rock or kg HC/ton of rock for PP and ± 0.1 mg HC/g of rock or kg HC/ton of rock for PI. The vitrinite reflectance (R_0), T_{max} and surface temperature measurements of Alif-1 well [27] and raw well log data were used in PetroMod 1D and Surfer 7 to generate burial history-maturity models and isopach maps of the Alif Sandstone reservoir.

4. Petroleum System

The petroleum system has been defined as the natural context through which related hydrocarbon accumulations are linked by origin and occurrences. A petroleum system includes all the elements and processes needed for an oil and gas accumulation to exist. Furthermore, it provides a link between the distribution of oil/gas and the stratigraphic and structural development in a basin. The Alif Sandstone Member is the main hydrocarbon reservoir of the Marib sub-basin, Block 18 oilfields (Fig. 2). The estimated reserve of the Block 18 oilfields is more than 900 MBO and 17 trillion cubic feet of natural gas [13 and 36].

The majority of oilfields and discoveries in the Sab'atayn Basin are associated with structural traps, but the potential for stratigraphic and combination traps is well-developed throughout the sedimentary succession. The most common structural traps in the Sab'atayn Basin are due to tilting of hanging-wall fault blocks, tilted-fault blocks, salt movement, differential compaction and drape anticlines ([13, 16, 22, 23 and 37]. During the Late Jurassic a gentle north-east extension resulted in low angle listric faults along a salt detachment, which, together with the salt seal, provide the trapping mechanism within the Marib sub-basin [23 and 37]. Salt and shale beds of the Sab'atayn Formation are serving as major seal rocks for most of the Sab'atayn Basin reservoirs (Fig. 2). These halite strata act as barriers against the vertical migration of petroleum and thus, are effective seal rocks.

The essential parts of the Marib sub-basin, Block 18 oilfields and its petroleum system consisting of source rocks, reservoirs and seals mainly occur in the Kimmeridgian-Tithonian sequences of the Madbi and Sab'atayn Formations (Fig. 2).

5. Source Rock Assessment

The Rock-Eval pyrolysis results of the Meem and Lam Members of the Madbi Formation existing in the Marib sub-basin, Block 18 oilfields, are used to evaluate the source rocks (Table 1). The organic-rich beds of the both Members serve as the main petroleum source rocks in the Sab'atayn Basin. Source rock assessments were based on methods described in

literature [30, 31, 32, 33, 38, 39 and 40].

5-1. TOC and Petroleum Potential

Rock-Eval pyrolysis is the most widely used method for determining the amount and type of organic matter in a potential source rock and for measuring its hydrocarbon potential [30 and 31]. TOC and Rock-Eval pyrolysis data and the parameters of the Madbi Formation are graphically represented in the organic geochemical log of the studied wells in Figure 3. The organic geochemical logs indicate the presence of good quality source rocks in all the studied wells, particularly within the Lam Member occurring in Alif-1, Meem-1, J. Haddan-1, Salah Al-Deen-1 and Al-1 wells (Figs. 3a-b; 3e-g). In addition, the organic geochemical logs indicate the presence of good quality source rocks within the Meem Member of the Madbi Formation in Kamaran-1 and Tawilah-1 wells (Figs. 3c-d). The studied samples of the Lam and Meem Member have fair to excellent TOC values (Table 1). According to many authors, sediments with TOC values of 0.5 to 1.0 wt% are considered as potential source rocks [38, 39, 40, 41 and 42]. The TOC contents of the Lam Member range from 0.12 to 5.97 wt% with an average value of 1.47 wt% and the PP contents vary from 0.16 to 31.52 mg HC/g of rock with an average value of 4.62 mg HC/g of rock (Table 1). The TOC contents of the Meem Member range from 0.3 to 12.34 wt% averaging 1.51 wt% and the PP contents range from 0.27 to 44.78 mg HC/g of rock with an average value of 4.34 mg HC/g of rock (Table 1). Most of the studied samples have fair to excellent petroleum potential (Figs. 4a-c).

Samples from some intervals have relatively high S2 and HI values, particularly samples from the depth interval 1085 m to 1270 m in a Tawilah-1 well (Fig. 3c). The highest TOC values reach 12.32 wt% within the Meem Member of the Madbi Formation in the Tawilah-1 well (Fig. 3c).

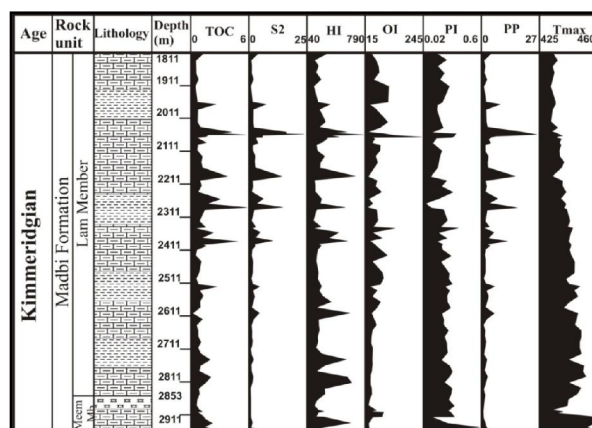


Fig. 3a. Organic geochemical log summarizing Rock-Eval pyrolysis/TOC results for the Madbi Formation of J. Haddan-1 well.

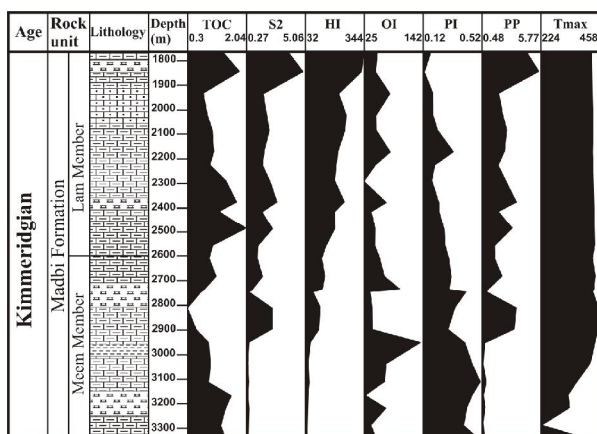


Fig. 3b. Organic geochemical log of Alif-1 well.

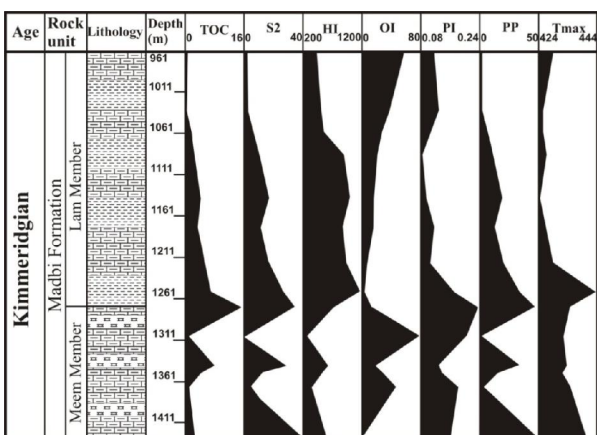


Fig. 3c. Organic geochemical log of Tawilah-1 well.

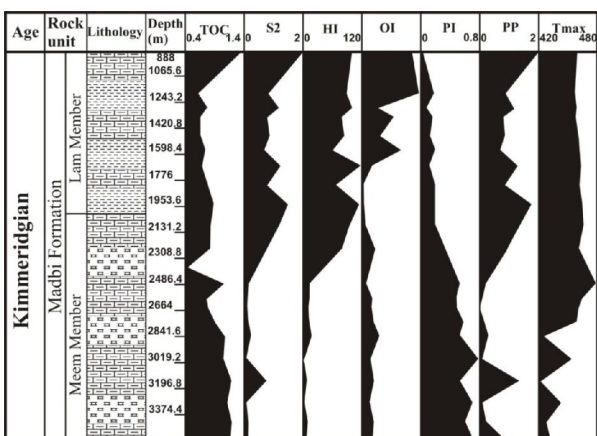


Fig. 3d. Organic geochemical log of Kamaran-1 well.

The PI results of most of the studied samples of the two Members show good hydrocarbon potentiality, particularly those of the Meem Member as they range from 0.04 to 0.69 kg HC/ton of rock with an average value of 0.33 kg HC/ton of rock. Results of the Lam Member show values ranging from 0.02 to 0.42 kg HC/ton of rock with a relatively lower average value of 0.21 kg HC/ton of rock.

TOC, PP and PI results of the seven studied wells as well as the data from the neighbouring wells [27] were used to construct TOC, PP and PI average concentration maps for the Madabi Formation by using Surfer 7 software program (Figs. 4d-f). Figure 4d indicates TOC anomalies at the Al-Raja, Dostour Al-Wahdah and Tawilah oil/gas fields of Block 18, at the Jannah and Halewah oil/gas fields of Block 5 and at the Rajwan-1 well of Block 75.

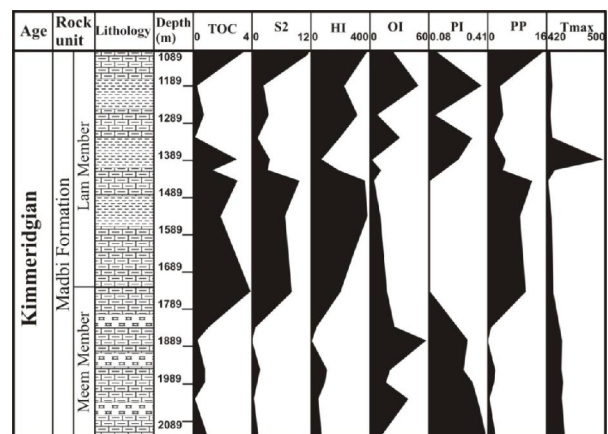


Fig. 3e. Organic geochemical log of Meem-1 well.

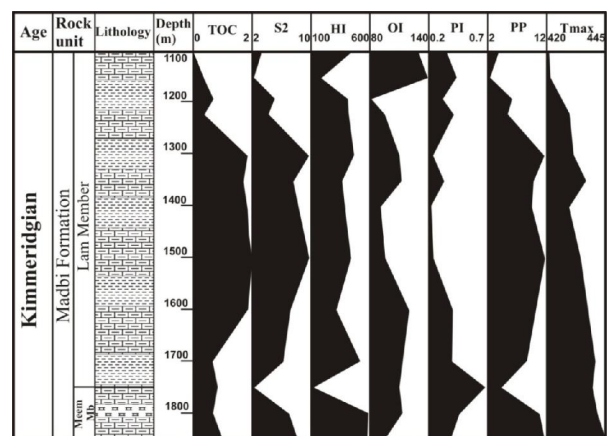


Fig. 3f. Organic geochemical log of AI-1 well.

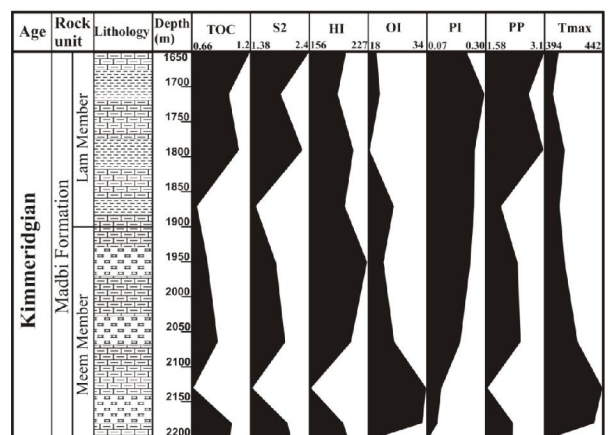


Fig. 3g. Organic geochemical log of Salah Al-Deen-1 well.

Figure 4e shows PP anomalies at the Al-Raja, Dostour Al-Wahdah and Halewah oil/gas fields of Block 18 and Block 5. Figure 4f indicates PI highs around the Kamaran-1, Alif-1, AI-1 and Halewah-1 wells of Block 18 and 5.

5-2. Kerogen Type and Maturity

In general, due to increasing molecular complexity, the T_{max} value interval is narrow for organic material of kerogen type I (organic matter from algae), wider for kerogen type II (mixed marine organic matter) and is much wider for kerogen type III (terrestrial organic matter) [41]. The maturation window for oil and condensate/wet gas generation from organic matter of kerogen type II ranges from 430 to 470°C within the catagenesis stage. Organic matter of kerogen type III may generate wet/dry gas within the early stage of metagenesis; however, generation of dry gas is associated with pyrolysis temperatures of 470°C to 500°C [31, 32, 33, 39, 40, 41 and 42].

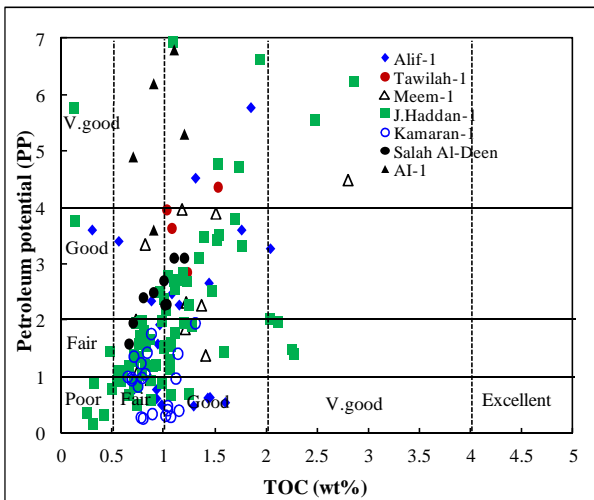


Fig. 4a. Plot of PP versus TOC displaying the generation potential of the studied samples.

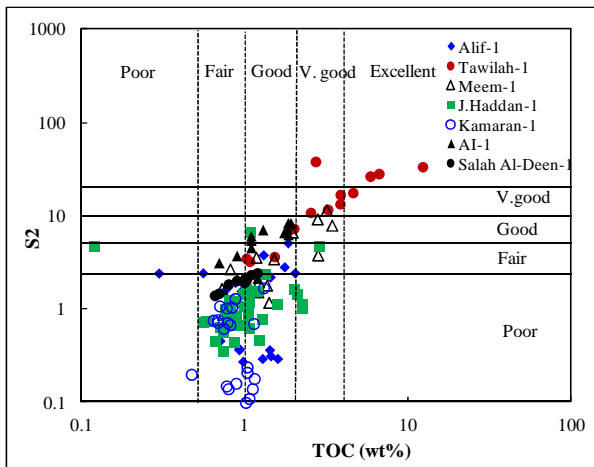


Fig. 4b. Plot of Rock-Eval S2 versus TOC of studied wells of the Madbi Formation.

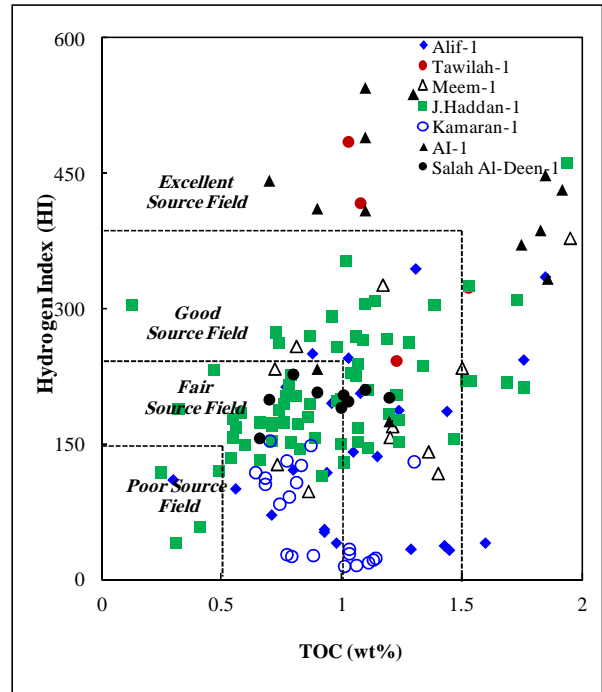


Fig. 4c. Plot of HI versus TOC for the Madbi Formation showing petroleum potential.

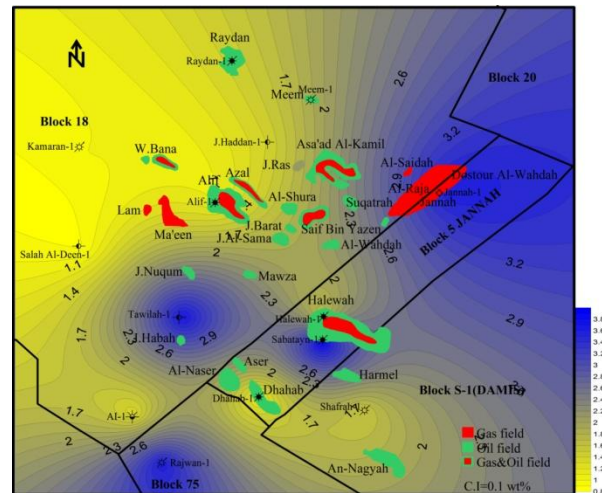


Fig. 4d. Average TOC concentration map of the Madbi Formation in the study area. Note that the figure displays TOC anomalies at the Al-Raja, Dostour Al-Wahdah and Tawilah oil/gas fields.

HI versus T_{max} and HI versus OI plots show that most of the studied samples are enriched in kerogen types II and III and largely depleted in kerogen type I (Figs. 5a-b). HI values of the Madbi Formation range from 16 mg to 1114 mg HC/g TOC with an average value of 273 mg HC/g TOC (Table 1). Meanwhile HI values of the Lam Member are greater than those of the Meem Member. They vary from 40 mg to 1114 mg HC/g TOC with an average value of 291 mg HC/g TOC whereas those of the Meem Member show values from 15 mg to 690 mg HC/g TOC with an average value of 184.8 mg HC/g TOC suggesting the presence of

kerogen types II and III. Kerogen type II content is greater than type III in the analyzed samples of the Lam Member whereas the samples of the Meem Member may show the reverse relationship.

The high values of HI within the depth interval between 1058m and 1270m of Tawilah-1 well indicate kerogen type I (Figs. 5a-b). High HI values are also recorded at depths of 2058m, 2060m, 2178m, 2282m, 2385m, 2605m, 2747m and 2800m to 2817m of J. Haddan-1 well and within the depth interval between 1800m - 1850m of AI-1 well (Table 1; Figs. 3, 5). These intervals of high HI values from three wells indicate the presence of kerogen type I.

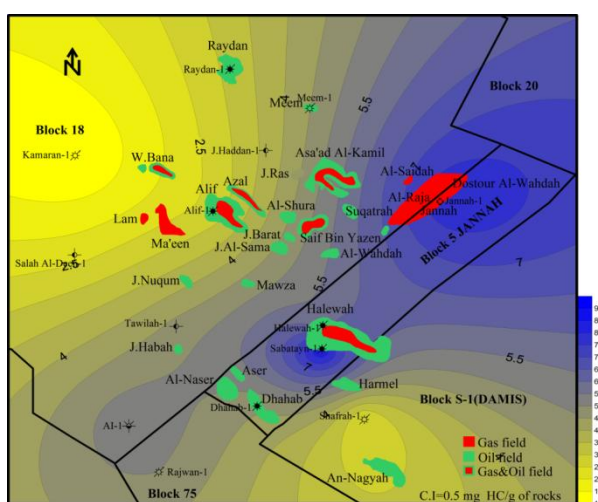


Fig. 4e. Average PP concentration map of the Madbi Formation in the study area. Note that the figure indicates PP anomalies at the Al-Raja, Dostour Al-Wahdah and Halewah oil/gas fields.

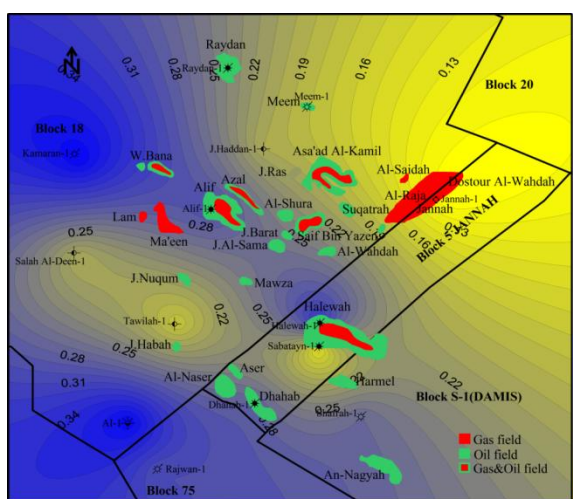


Fig. 4f. Average PI concentration map of the Madbi Formation in the study area. Note that the figure shows highs around the Kamaran-1, Alif-1, AI-1 and Halewah-1 wells of blocks 18 and 5.

T_{max} results show that most of the studied samples of the two Members are within the catagenesis stage,

particularly those of the Lam Member as they range from 400 to 482 °C with an average value of 436.34 °C. Samples of the Meem Member vary between the immature and the peak of the mature stage and range from 224 to 474 °C with an average value of 423.91 °C (Table 1, Figs. 5a and 6a-b).

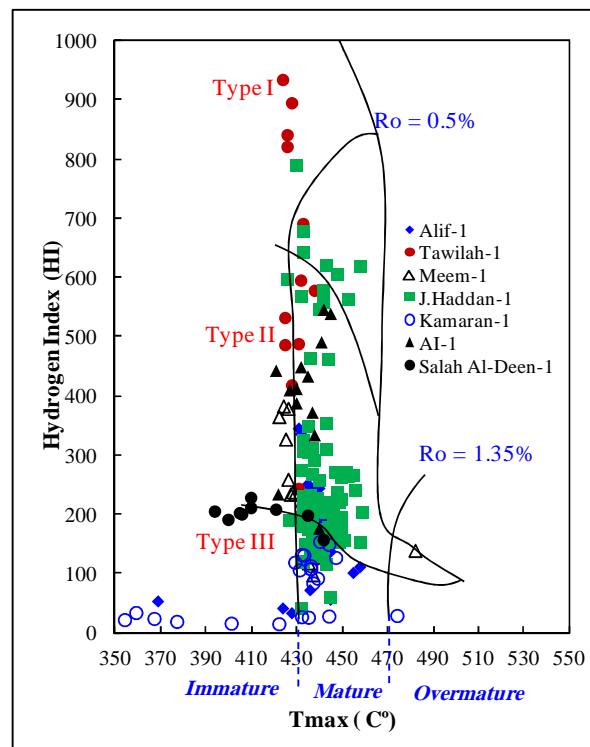


Fig. 5a. Plot of HI versus T_{max} indicating kerogen types and maturation stages.

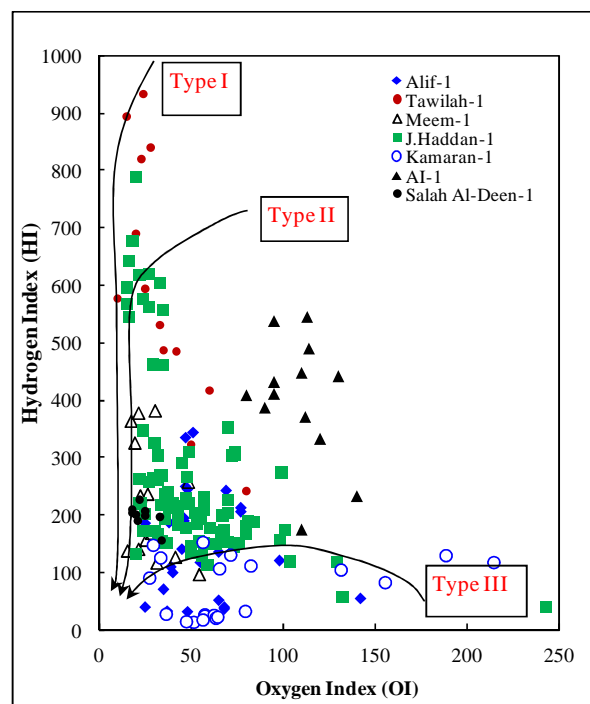


Fig. 5b. Plot of HI versus OI displaying kerogen types and maturation stages.

The T_{max} results of the studied wells and available T_{max} data from the neighbouring wells [27] were used to generate a map of the T_{max} distribution in the study area (Fig. 6b). This figure indicates anomalies of T_{max} in the northern, central and south-western parts of the Block 18 at the Raydan, Meem, As'ad Al-Kaml, J. Habah oil/gas fields as well as at the wells of AI-1 and at the Tawilah-1 extending into the southern part of Block 5 and down to the An-Nagyah oilfield in Block S1.

5-3. Generation Potential

The generation potential (GP) of the studied Madbi Formation samples is represented in organic geochemical logs (Figs. 3a-g). These logs indicate preservation of sufficient organic matter within the Lam and Meem Members of the Madbi Formation to qualify them as potential source rocks within the Marib sub-basin.

Most of the studied samples of these two Members have good TOC values with an average value of 1.48 wt%, a maximum value of 12.34 wt%, good PP contents averaging 4.54 kg HC/ton of rock and a maximum value of 44.78 kg HC/ton of rock (Table 1; Figs. 4a, 4d-e).

In general, hydrocarbon generation depends on good quantity and quality of organic matter and maturation. Commonly the high contents of type II kerogen in the studied samples may indicate that the Lam and Meem Members are at the peak of oil generation. This is supported by using a T_{max} versus PI plot [40 and 43] (Fig. 6a) and by using further relations of pyrolysis indicators with other parameters (Figs. 4-6a-b). Results are presented in HI versus T_{max} and T_{max} versus PI diagrams (Figs. 5a; 6a). These plots indicate the presence of large amounts of kerogen types II, III and less amount of kerogen type I which are mostly mature thermally and have potential to generate oil and gas.

Hydrocarbon expulsion from the Madbi Formation source rocks may have commenced during the Early Cretaceous and continued until the Tertiary which is associated with the vast floods of lava erupted during the Red Sea and Gulf of Aden rifting.

5-4. Reservoir

The Alif Sandstone Member of the Sab'atayn Formation, together with the other minor reservoir sandstones within the Yah, Seen and Safer Members of the Sab'atayn Formation, are the main reservoir in the Block 18 oilfields (Fig. 2). Additionally, the fractured/weathered basement rocks viz. Kuhlan and Madbi Formations act also as minor to major reservoir units in the neighbouring productive blocks as S1 and 20 of the Sab'atayn Basin (Figs. 1-2). The Alif Member is mainly composed of sandstones accumulated in braided fluvial, braided delta/plain and

shallow-nearshore marine depositional environments [13, 21 and 27]. Most of the reservoir sandstones of the Alif Member are composed mainly of quartz arenites or subarkoses together with rare lithic arenites [13 and 27].

Isopach maps of the Alif Sandstone Member were constructed from the raw data base of the studied and neighbouring wells, well-logs and drilling reports as well as from the internal reports of the Petroleum Exploration and Production Authority-Yemen (PEPA) and from the oil companies working in the Sab'atayn Basin (Figs. 7a-b). Figure 7a shows a thickness distribution map of the Alif Sandstone Member in the studied area indicating its progressive thickening toward the eastern and western direction of the Block 18. The first of the two strong anomalies is located around the Dostour Al-Wahdah oilfield with an average thickness of 380m in the east whereas the second one occurs at the Alif, Azal, Lam, Ma'een, W. Bana, and J. Nuqum oil/gasfields with a thickness ranging between 200m to 240m in the west. This easterly thickening of the Block 18 extends toward Block 5 at the Jannah gasfield and the Block 20 (Fig. 7a). Thinning of the Alif Sandstone Member occurs toward the northern direction at Raydan oilfield with an average thickness of 140m, in the central and southern parts of the Block 18 oilfields, the Suqatrah, the Saif Bin Yazan and the Al-Wahdah oilfields (with an average thickness of 120m) toward the Halewah oilfield of Block 5 (Fig. 7a).

These two anomalies of the Alif Sandstone thickness in the study area may result from the asymmetric arrays of horst and graben structures dissecting the stretched region where the basin-filling sediments are generally deposited above the down-dropped and tilted fault blocks. Figure 7b represents the distribution of the upper surface depths of the Alif Sandstone Member within the study area which shows three depths of anomalies. These anomalies extend from ENE to WSW and are parallel to the Gulf of Aden Rift. The first deeper anomaly is located at the Al-Saidah and the Al-Raja gas fields reaching depths of 2800m (Fig. 7b). The second one lies at the Al-Wahdah oilfield with a depth of 2100m (Fig. 7b). The third anomaly occurs around the J. Nuqum oilfield with depths reaching up to 2000m (Fig. 7b).

The depth differences may also have arisen from the rejuvenation of horst and graben movements associated with the reactivation of weak lineaments of the basement blocks along the NE-SW direction of the Marib sub-basin rift events during the Late Jurassic time (Fig. 7b). Syn-sedimentary growth faulting along the NW-SE trending listric faults appears to have been important in controlling the thickness and type of facies of the Alif Sandstone in the Marib sub-basin and the Block 18 oilfields [13, 18 and 27].

The Block 18 oilfields produced from depths as shallow as 1000m to as deep as 3000 meters. Total

hydrocarbon column thicknesses of the discovered fields vary from a few meters to more than 975m of vertical relief. The fields also vary in areal size from 0.4 km² (100 acres) to approximately 57km² (14000 acres). Reservoir quality of the Alif Sandstone is excellent with a macroporosity (>16µm) often ranging between 18 and 24% with an additional microporosity (<16µm) of 1-2% [13].

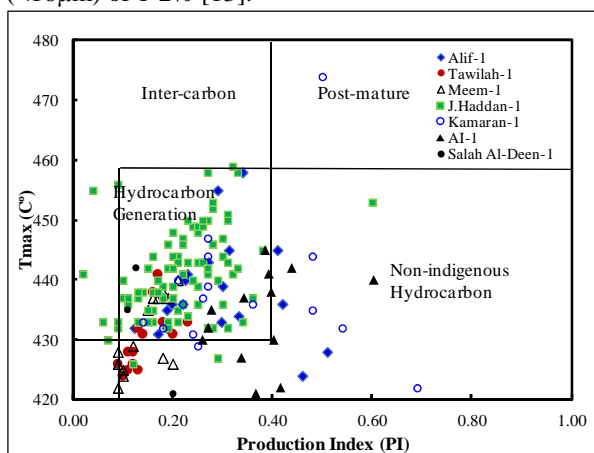


Fig. 6a. GP plot of T_{max} versus PI showing that the majority of the studied samples are located within the hydrocarbon generating zone.

values, used as calibration parameter, could be achieved by assuming an erosion of 1100 m of the Upper Tawilah group overburden from the Middle to Late Paleogene, a constant heat flow of 60 mW/m² and a heat flow peak due to the onset of basin rifting in Late Jurassic of 90 mW/m². Thus, the Lam Member at its deepest burial has reached the main oil to wet gas window whereas the Meem Member in its full thickness has undergone the wet gas window (Figs. 8b).

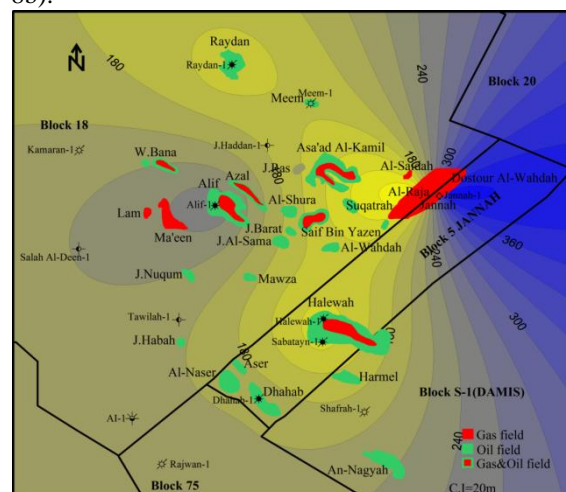


Fig. 7a. Isopach thickness map of the Alif Member (the main reservoir of Block 18 oilfields).

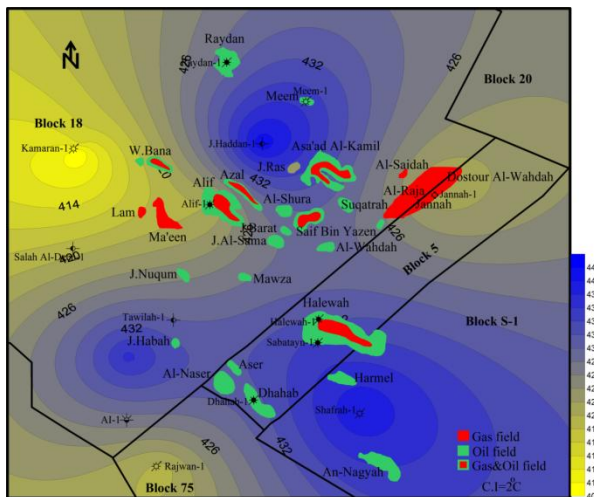


Fig. 6b. Average T_{max} distribution map of the Madbi Formation in the study area.

6. Modelling Results

Vitrinite reflectance (R_0) measurements of the Alif-1 well were used to calibrate the maturity and burial history of this well representing the general burial history trend of the study area by using the PetroMod software suite (Schlumberger[®]) (Table 2; Figs. 8a-e). The calculated temperature for the time of deepest burial of the Madbi Formation source rock layers reached 158°C for the Lam Member and 182°C for the Meem Member (Fig. 8a-1). Compliance with R_0

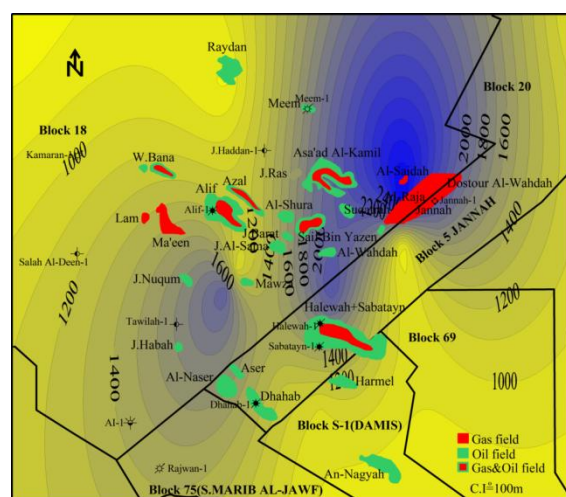


Fig. 7b. The upper surface depth of the Alif Member belonging to Sab'atayn Formation.

6-1. Radiogenic Heat Production

The decay of radioactive isotopes in rocks and minerals implies the emission of energetic α - and β -particles, neutrinos and antineutrinos and γ -rays [44]. Neutrinos and antineutrinos are without mass or charge, almost transparent and the energy carried by them is transmitted into space. However, α - and β -particles do interact with the surrounding rocks which absorb their kinetic energy whereby heat is generated [44].

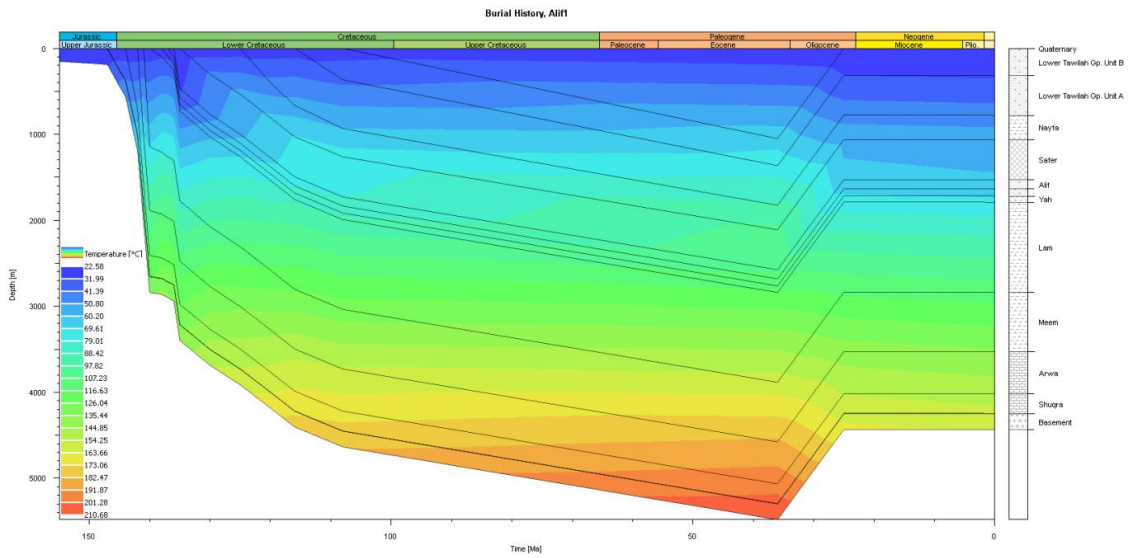


Fig. 8a-1. Burial history-temperature model of Alif-1 well.

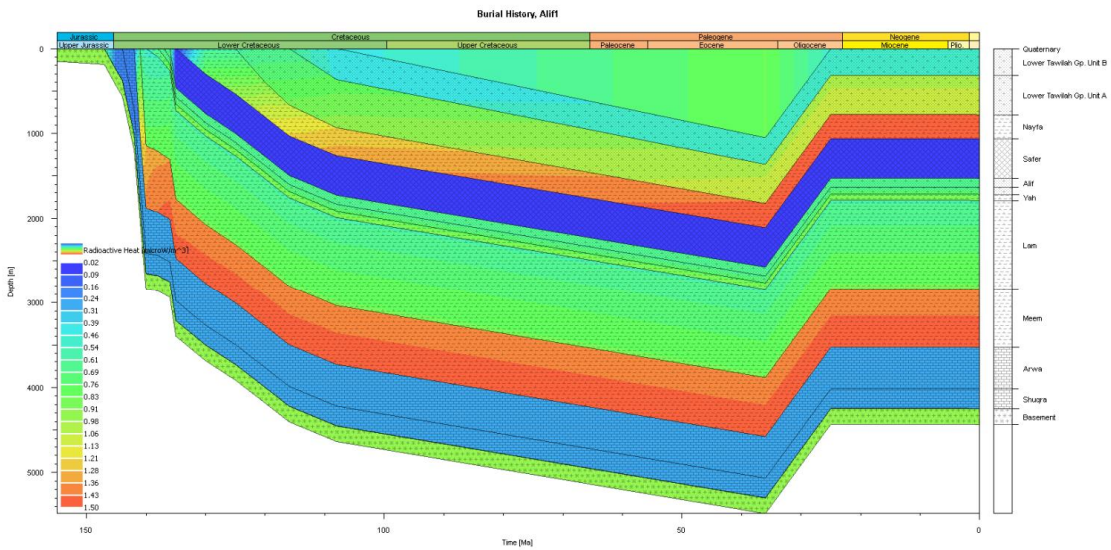


Fig. 8a-2. Burial history-radioactive heat model of Alif-1 well.

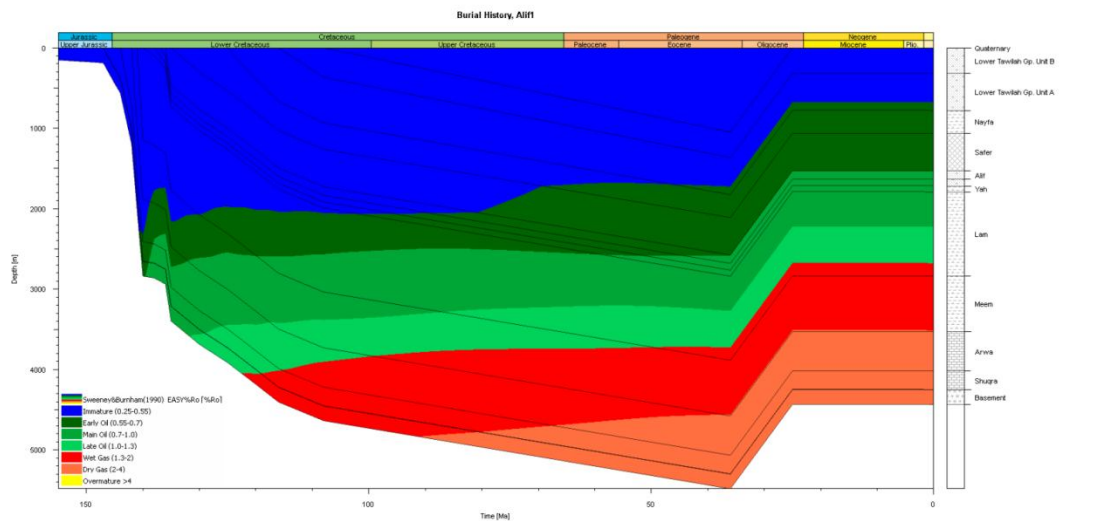


Fig. 8b. Burial history-maturity model of Alif-1 well.

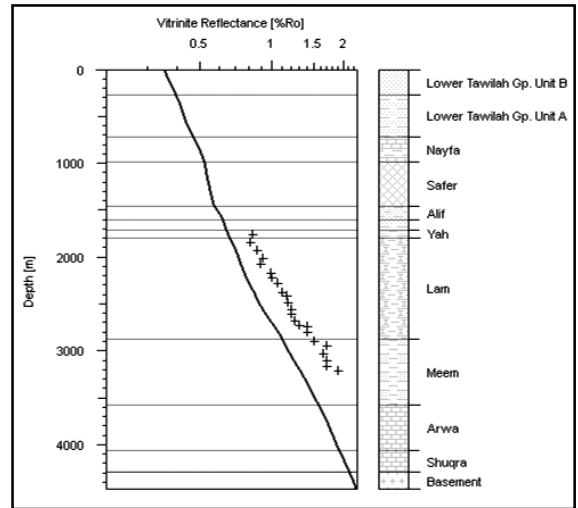
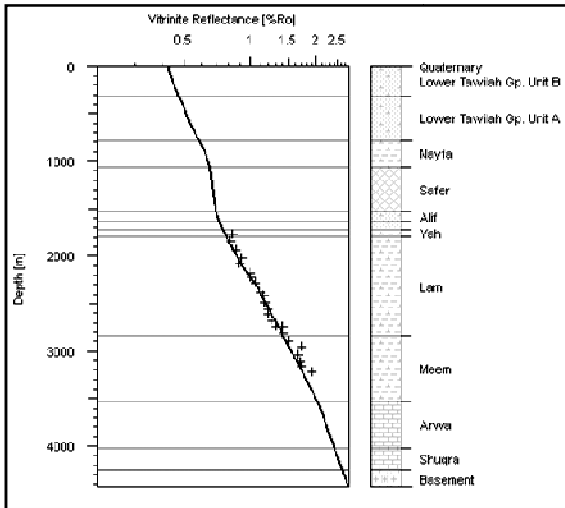


Fig. 8c. Modelling results of Alif-1 well considering (left) or neglecting (right) radiogenic heat production of the basin infill.

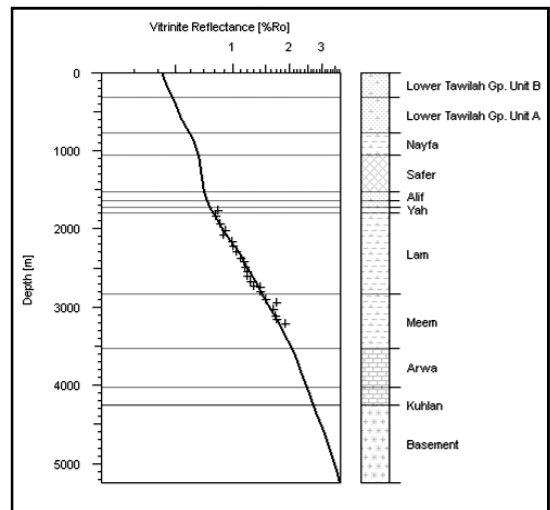
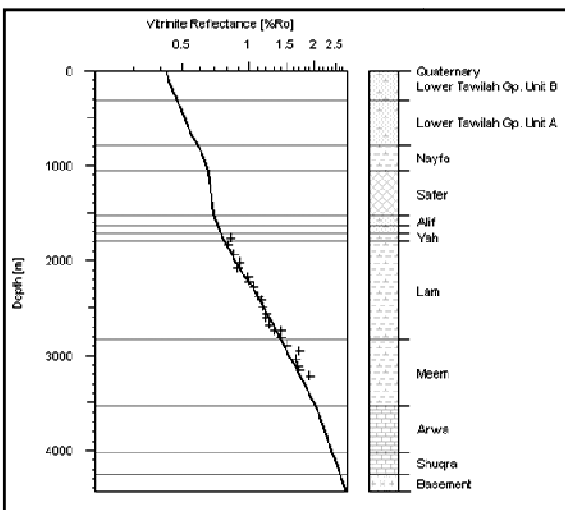


Fig. 8d. Modelling results of Alif-1 well for a basement thickness of 183m (left) and 1000m (right).

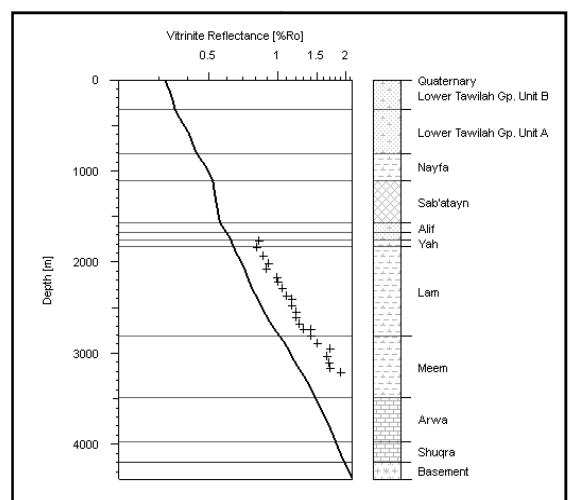
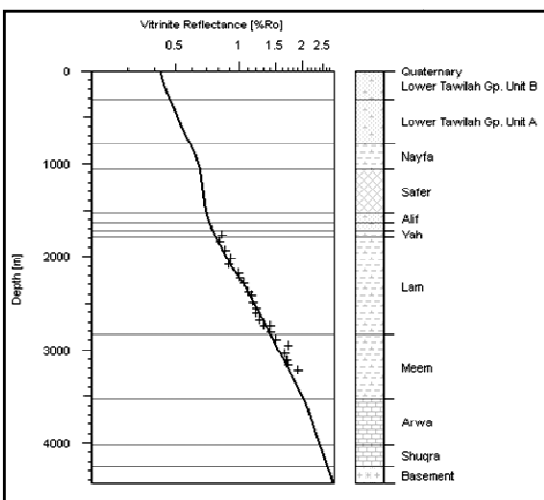


Fig. 8e. Modelling results of Alif-1 well for a single erosion event of 1100m (left) and 1100m split into several events (right).

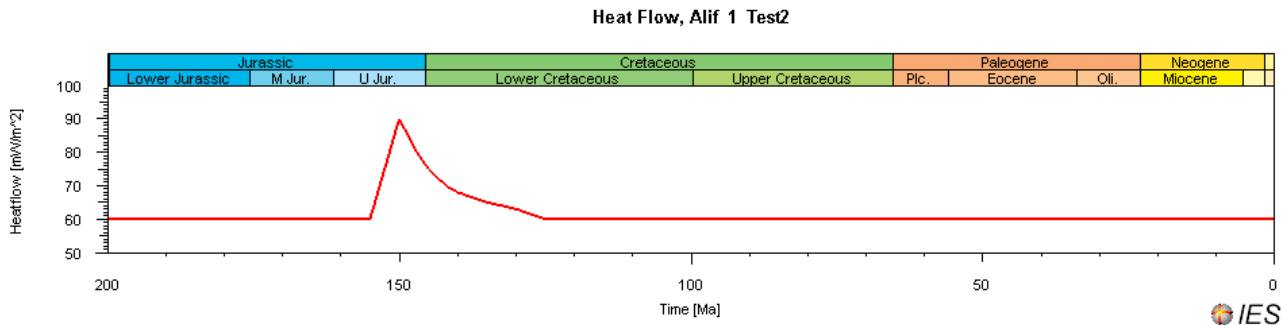


Fig. 8f. Paleo heat flow through time.

This radiogenic heat production was taken into account in this simulation approach posing an essential novelty with respect to the modelling process (Fig. 8a-2). Figure 8c illustrates the significant influence of the radiogenic heat production. The modelling results obtained for the Alif-1 well depend on whether we consider (right) or ignore this heat production (left). A good fit for the model where radiogenic heat production was not considered could only be achieved by increasing the heat flow base line by 8mW/m².

6-2. Basement Thickness

Due to the fact that only little or no exact information about the basement thickness is available this parameter is frequently a part of the underlying assumptions or interpolations and should be considered highly speculative. However, Fig. 8d reveals that the variation of basement thickness with its internal radiogenic heat production involves only minor neglectable impacts on modelling results even though the basement thickness has been increased from 183 m to 1000 m in this example. It shows a slightly elevated calculated maturity but with the assumed radiogenic heat production of 1 microW/m³ significantly larger basement thicknesses would be needed for a considerable increase of the calculated maturity.

6-3. Erosion

The process of erosion which is mostly accompanied by uplift events is of crucial importance for the trend of the qualification gradient. While varying the erosional thicknesses is a common approach for calibrating the numerical models, the exact amount still remains speculative. In order to test the sensitivity regarding erosion the amount of 1100 m erosional thickness has been split into several events according to known unconformities (Top of the Tawilah Group, Top of the Nayfa Formation, Top of the Madbi Formation and Top of the Kuhlan Formation). Cretaceous and Tertiary sediments were eroded after uplift related to the Red Sea rifting which has been estimated as 1000 m in the Marib sub-basin [37]. Figure 8e shows that the splitting of the erosional thickness results in a decline in the calibration match. A good fit between the measured and calculated R_0

values would then require an additional major increase of erosional thickness and/or basal heat flow (Figs. 8e).

6-4. Heat Flow

The heat flow is one of the most essential parameters affecting the temperature gradient of a numerical model [44]. For the Alif-1 well a paleo heat flow having its peak during Late Jurassic 90 mW/m² with a base line of 60 mW/m² has been applied successfully. This peak is related to the initial rifting event which started the basin development (Fig. 8e). Since calibration values are only present for the post-rift basin fill the heat flow peak does not influence the model calibration and only displays the characteristic minimum heat flow regime of a rifting event (90-115 mW/m²) (Fig. 8f).

Table 2. Vitrinite reflectance (R_0) and T_{max} results of Alif-1 well, Block 18 oilfields, Sab'atayn Basin.

Formation	Member	Sample No.	Depth (m)	R_0 (Avg.)	No. of meas.	T_{max} °C
MADBI	LAM	1	1764	0.83	13	431
		2	1844	0.81	14	432
		3	1932	0.86	14	432
		4	2020.5	0.91	13	435
		5	2082	0.89	18	436
		6	2170.5	0.99	17	434
		7	2223.5	1	13	436
		8	2288	1.05	13	437
		9	2376	1.1	17	440
		10	2414.7	1.15	13	441
		11	2485	1.16	17	443
		12	2555.8	1.2	13	443
		13	2608	1.2	14	443
		14	2682	1.25	15	445
	MEEM	15	2735	1.3	14	439
		16	2742.6	1.4	12	436
		17	2808.8	1.4	22	448
		18	2897	1.5	14	449
		19	2950	1.7	23	445
		20	3038	1.65	15	425
		21	3111.7	1.69	15	380
		22	3164.7	1.7	16	370
		23	3217.6	1.9	14	340

7. Conclusion

Our data of Rock-Eval pyrolysis analysis of 183 samples from seven wells of the Lam and Meem members in the Madbi Formation as well as the isopach maps of the Alif reservoir unit and the basin modelling results in the Block 18 oilfields, Sab'atayn Basin, allow the following concepts to be drawn:

1. Most of the studied samples of the two members have good TOC values with an average value of 1.48 wt%, a maximum value of 12.34 wt% and good PP contents with an average value of 4.54 kg HC/ton of rock and a maximum value of 44.78 kg HC/ton of rock. The TOC contents of the Lam Member range from 0.12 to 5.97 wt% with an average value of 1.47 wt% and the PP contents vary from 0.16 kg to 31.52 kg HC/ton of rock with an average value of 4.62 kg HC/ton of rock. The TOC contents of the Meem Member range from 0.3 to 12.34 wt% with an average value of 1.51 wt%. The PP contents range from 0.27 kg to 44.78 kg HC/ton of rock with an average value of 4.34 kg HC/ton of rock.

2. PI results indicate that most of the studied samples of the two Members are good; particularly those of the Meem Member which range from 0.04 kg to 0.69 kg HC/ton of rock with an average value of 0.33 kg HC/ton of rock. The PI values of the Lam Member are relatively low and vary from 0.02 kg to 0.42 kg HC/ton of rock with an average value of 0.21 kg HC/ton of rock.

3. T_{max} data show that most of the studied samples of the two Members are within the mature stage (catagenesis stage); particularly those of the Lam Member which range from 400 to 482°C with an average value of 436.34°C. The samples of the Meem Member are immature to late-mature with T_{max} varying from 224 to 474°C with an average value of 423.91°C.

4. HI values of the Madbi Formation range from 16 to 1114 mg HC/g TOC with an average value of 273 mg HC/g TOC. According to the HI and OI results, the kerogen type II content is greater than type III in the Lam Member. By contrast the Meem Member shows kerogen type III contents being greater than type II.

5. The isopach map of the Alif Sandstone Member in the studied area indicates more thickening towards the eastern and western parts of the Block 18 oilfields. The first one of the two strong anomalies is concentrated around the Dostour Al-Wahdah oilfield having an average thickness of 380m in the east. This extends into the Block 5 at the Jannah gasfield and the Block 20. The second one is located near the Alif, Azal, Lam, Ma'een, W. Bana and J. Nuqum oil/gas fields with a thickness ranging from 240m to 200 m in the west.

6. Basin modelling results show that the calculated temperatures for the time of deepest burial of the Madbi Formation source rock layers reach 158°C for the Lam Member and 182°C for the Meem Member. The R_0 data and maturity modelling results indicate that the Lam Member has reached the main oil to wet

gas window whereas the Meem Member has undergone the wet gas window.

Acknowledgements

The first author thanks the Petroleum Exploration and Production Authority-Republic of Yemen, former Yemen Hunt Oil Company and Jannah Hunt Oil Company for providing samples and raw data upon which the present work was carried out. Deep thanks for my colleagues from Taiz University for their assistance during this study. We thank Dr. Habib Mollaei and IJES editorial staff. Deep thanks to referees Prof. Drs. Thamer Al-Ameri; Ali Khudeir and Mohammed Al-Wosabi for constructive comments which greatly improved the manuscript.

References

- [1] Lamare, P., 1930, Nature et extension des depots secondaires dans l'Arabie, l'Ethiopie et le pays Somalis. *Memoirs de la Société Géologique de France*, v. 14, p.49-68.
- [2] Lamare, P., Basse, E., Dreyfus, M., Lacroix, A. and Teilhard de Chardin, P., 1930, Etudes géologiques en Ethiopie, Somalie et Arabie méridionale. *Soc. Géol. France Mem. New Ser.*, v. 6(14), p. 1-83.
- [3] Geukens, F. P., 1960, Contribution à la géologie du Yemen. *Mémoires Institut Géologique de Louvain*, v. 21, p.122-179.
- [4] Geukens, F. P., 1966, Contribution to "Geology of Arabian Peninsula: Yemen". USGS Prof. Paper, Part 560-B, p.1-23.
- [5] Beydoun, Z. R., 1964, The stratigraphy and structure of the Eastern Aden Protectorate. *Overseas Geology Mineral Resources Bull. Supp.*, v. 5, p.1-107.
- [6] Beydoun, Z. R., 1966, Geology of the Arabian Peninsula; Eastern Aden Protectorate and Part of Dhufar. USGS Prof Paper 560-H, p.1-49.
- [7] Beydoun, Z. R. and Greenwood, J. E., 1968, Aden Protectorate and Dhufar, in *Lexique Stratigraphique International Vol. III., Asie*, L. Dubertret, (ed.), CNRS, Paris, Fasc.1062.
- [8] El-Nakhal, H. A., 1987, A lithostratigraphic subdivision of the Kuhlhan Group in Yemen Arab Republic. *Iraqi J. Sci.*, v. 28, p.149-180
- [9] El-Nakhal, H. A., 1988, Stratigraphy of the Tawilah Formation (Cretaceous-Paleocene) in the Yemen Arab Republic. *Ain Shams Univ., Earth Sci.*, v. 2, p.161-171.
- [10] El-Nakhal, H. A., 1990, Surdud Group, a new lithostratigraphic unit of Jurassic age in the Yemen Arab Republic. *J. King Saud Univ.*, 2, p.125-143.
- [11] Hughes, G. W. and Beydoun, Z. R., 1992, The Red Sea-Gulf of Aden: biostratigraphy, lithostratigraphy and paleoenvironments, *Journal of Petroleum Geology*, v. 15, p.135-56.
- [12] Bott, W. F., Smith, B. A., Oakes, G., Sikander, A. H. and Ibrahim, A.I., 1992, The tectonic framework and regional hydrocarbon prospectivity of the Gulf of Aden, *Journal of Petroleum Geology*, v. 15, p.211-243.
- [13] Taheri, A. A., Sturgess, M., Maycock, I., Mitchell, G., Prelat, A., Nurmi, R. and Petricola, M., 1992, Looking for Yemen's hidden treasure. *Middle East Well Evaluation Review-Schlumberger*, v. 12, p.12-29.

- [14] Beydoun, Z. R., Bamahmoud, M. O. and Nani, A. S., 1993, The Qishn Formation, Yemen: lithofacies and hydrocarbon habitat. *Marine and Petroleum Geology*, v. 10, p.364-372
- [15] Redfern, P. and Jones, J. A., 1995, The interior rifts of the Yemen-analysis of basin structure and stratigraphy in a regional plate tectonic context: *Basin Res.*, v. 7, p.337-356.
- [16] Ellis, A. C., Kerr, H. M., Cornwell, C. P. and Williams, D. O., 1996, A tectonostratigraphic framework for Yemen and its implications for hydrocarbon potential. *Petroleum Geoscience*, v. 2, p.29-42
- [17] Fantozzi, P. L., 1996, Transition from continental to oceanic rifting in the Gulf of Aden: structural evidence from field mapping in Somalia and Yemen. *Tectonophysics*, v.259, p.285-311
- [18] Beydoun, Z. R., As-Saruri, M. L. and Baraba, R. S., 1996, Sedimentary basins of the Republic of Yemen: their structural evolution and geological characteristics. *Rev. Inst. Fr. Pétrole*, v. 51(6), p.763-775.
- [19] Bosence, D. W., 1997: Mesozoic rift basins of Yemen. *Marine and Petroleum Geology*, v. 14(6), p.611-616.
- [20] Touché, F., Vidal, G. and Gratier, J. P., 1997, Finite deformation and displacement fields on the southern Yemen margin using satellite images, topographic data and a restoration method. *Tectonophysics*, v. 281, p. 173-193
- [21] Beydoun, Z. R., As-Saruri ML, El-Nakhal H, Al-Ganad IN, Baraba RS, Nani AS and Al-Aawah M. H., 1998, Republic of Yemen-International Lexicon of stratigraphy. Vol.III, Asia, fascicule 10b2. IUGS Publication No. 34, 245pp
- [22] Brannan, J., Sahota, G., Gerdes, K. D. and Berry, J. A. L., 1999, Geological evolution of the central Marib-Shabwah Basin, Yemen. *GeoArabia*, v. 41, p.9-34.
- [23] Seaborne, R. T., 1996, The influence of the Sab'atayn Evaporites on the hydrocarbon prospectivity of the Eastern Shabwah Basin, Onshore Yemen. *Marine and Petroleum Geology*, v.13, p.963-912.
- [24] Csato, I., Habib, A., Kiss, K., Koncz, I., Kovács, Z., Lrincz, K. and Milota, K., 2000, Play concepts of oil exploration in Yemen, *Oil and Gas Journal*, v. 99, p.68-74.
- [25] Worden, R. H., 2005, Dawsonite cement in the Triassic Lam Formation, Shabwah Basin, Yemen: A natural analogue for a potential mineral product of subsurface CO₂ storage for greenhouse gas reduction. *Marine and Petroleum Geology*, v. 23, p.61-77
- [26] Shinaq, R., Al-Matary, A., Al-Taani, A. A. and Mahasneh, M., 2010, Evaluation of Middle-Upper Jurassic Source Rocks (Amran Group) in Sabatayn Basin, Yemen, *Africa Geoscience Review*, v.17 (3), p.157-174.
- [27] Alaug, A. S., 2002, Source Rocks Evaluation and Palynofacies of Late Jurassic-Early Cretaceous Succession of Marib-Shabwah Basin, Republic of Yemen. PhD Unpublished Thesis, University of Baghdad-Iraq, 295pp.
- [28] Al-Thour, K. A., 1997, Facies sequences of the Middle-Upper Jurassic carbonate platform (Amran Group) in the Sana'a region, Republic of Yemen. *Marine and Petroleum Geology*, v.14(6), p.643-660.
- [29] Mitchell, G. and Kohles, K. M., 1995, Depositional sequences in the Upper Jurassic of the Marib-Jawf Basin, Republic of Yemen. In: *Rift sedimentation and tectonics in the Red Sea-Gulf of Aden region* (Ed. D. W. J. Bosence) Abst. Vol., Sana'a, Yemen, p.44.
- [30] Espitalie, J., Laporte, J., Madec, M., Marquis, F., Leplat, P., Paulet, J. and Boutefeu, A., 1977, Rapid method for characterization the petroleum potential and degree of evolution of source rocks. *Revue de l'Institut Français du Pétrole*, v. 32, p.23-42.
- [31] Espitalie, J., Deroo, G. and Marquis, F., 1985, La pyrolyse Rock-Eval et ses applications. Partie I. *Rev. Inst. Fr. Pétrole*, v. 40(5), p.563-579.
- [32] Peters, K. E., 1986: Guidelines for evaluating petroleum source rock using programmed pyrolysis. *American Association of Petroleum Geologists Bulletin*, v.70, p.318-329.
- [33] Peters, K. E. and Cassa, M. R., 1994, Applied source rock geochemistry. In: Magoon, L. B. and Dow W. G. (eds): *The petroleum system—from source to trap*. American Association of Petroleum Geologists-Memoir, v. 60, p. 93-120.
- [34] Lafargue, E., Marquis, F. and Pillot, D., 1998, Rock-Eval 6 applications in hydrocarbon exploration, production and soils contamination studies. *Oil & Gas Sci. Technol. Rev. IFP*, 53 (4), p.421-37
- [35] Behar, F., Beaumont, V. and De B Penteadó, H. L., 2001, Rock-Eval 6 technology: performances and developments. *Oil & Gas Sci. Technol. Rev. IFP* 56(2), p.11-134
- [36] Webster, R. L., Wharton, R. J, Isaksen, G. H, Clendenen, W. S. and Talukdar, S. C., 1995, Lam/Meem-Alif Petroleum System of the Marib-Jawf Basin, Republic of Yemen. In: Bosence, D. (ed.), *Rift sedimentation and tectonics in the Red Sea- Gulf of Aden region*. Abs. Vol. p. 81
- [37] Mitchell, G. and Galbiati, L. D., 1995, Tectonic and stratigraphic framework of the Marib-Jawf Basin, Yemen. In: *Rift sedimentation and tectonics in the Red Sea-Gulf of Aden region* (Ed. D. W. J. Bosence), Abstract volume, Sana'a, Yemen, p.43.
- [38] Tissot, B. P. and Welte, D. H., 1984, *Petroleum Formation and Occurrence*, 2nd ed. Springer, New York, 699 pp.
- [39] Bordenave, M. L., 1993, *Applied Petroleum Geochemistry*. Editions Technip, Paris, 425pp.
- [40] Hunt, J. M., 1996, *Petroleum geochemistry and geology*, 2nd ed. Freeman, New York, 743pp.
- [41] Tissot, B. P., Pelet, R. and Ungerer, P. H., 1987, Thermal history of sedimentary basins, maturation indices and kinetics of oil and gas generation. *AAPG Bull.*, v. 71, p.1445-1466.
- [42] Killops, S. D. and Killops, V. J., 1995, *Introduction to organic geochemistry*. Sec. Edit: Blackwell, 393pp.
- [43] Langford, F. F. and Blanc-Valleron, M. M., 1990, Interpreting Rock-Eval pyrolysis data using graphs of Pyrolizable hydrocarbons vs. total organic carbon. *American Association of Petroleum Geologists Bulletin*, v. 74, p.799-804.
- [44] Hantschel, T. and Kauerauf, A. I., 2009, *Fundamentals of Basin and Petroleum Systems Modelling*, Springer-Verlag Berlin Heidelberg, 476 pp.
- [45] As-Saruri, M. L., Sorkhabi, R. and Baraba, R., 2010, Sedimentary basins of Yemen: their tectonic development and lithostratigraphic cover. *Arabian Journal of Geosciences-v.3*, p.515-27.